

Investigating the Effects of Fused Deposition Modeling Parameters on Carbon Fiber-Reinforced PLA Performance

Manel Dhouioui¹, Boutheina Ben Fraj², Wissem Zghal³, Hamdi Hentati^{1,4*}, Mounir Ben Amar⁵, Mohamed Haddar¹

¹Research Laboratory of Mechanics, Modeling and Manufacturing, National Engineering School of Sfax, University of Sfax, Tunisia

²Nanomaterials and Systems for Renewable Energy Laboratory, Research and Technology Center of Energy, TechnopoleBorjCedria, HammamLif, Tunisia.

³High institute of Industrial Management of Sfax, University of Sfax, Tunisia

⁴High School of Sciences and Technology of Hammam Sousse, University of Sousse, Sousse, Tunisia

⁵Laboratoire des Sciences des Procédés et des Matériaux, CNRS, Université Sorbonne Paris Nord, Villetaneuse, France

Received 7 Apr 2025

Accepted 31 Jul 2025

Abstract

In our work, the influence of the printing speed, the raster angle, the layer thickness, and the short carbon fiber-reinforced composites based on PLA as matrix on the thermal, mechanical, and microstructural properties were analyzed. These composites were printed using as 3D printing process the fused deposition modeling (FDM). To ensure the reliability of the experimental results, three measurements were elaborated on each tensile and micro-hardness test condition and the average values are used. Standard deviation (SD) was calculated to provide statistical validation of our experimental results. Based on tensile measurements, the raster angle $\theta = 0^\circ$ considerably increases stiffness and strength, mainly in thinner layers ($T_h = 0.3\text{mm}$). In fact, increasing T_h from 0.3mm to 0.4mm leads to a significant improvement in the stiffness of the printed parts, with the increase of Young's modulus (E) reaches up to 250%. Additionally, the higher printing speed increases strength of printed composites whereas decreasing their stiffness. In fact, a higher printing speed increases the strength of the printed composites, with the ultimate tensile strength (UTS) increasing by 90%, whereas it decreases their stiffness, with the Young's modulus (E) dropping by 15%. Furthermore, adding short carbon fibers into the polymer matrix significantly advances the stiffness and the strength of printed composites (SCFR-PLA) compared to printed polymer (PLA). However, this improvement is accompanied with a decrease of ductility of printed parts. These results provide appreciated understandings into optimizing 3D printing parameters for improved properties of printed composites in various engineering applications. Furthermore, thermogravimetric analysis (TGA) and scanning electron microscopy (SEM) were developed to analyze respectively the thermal behavior of printed composites (SCFR-PLA) and the relationship between porosity of printed parts and their mechanical properties.

© 2025 Jordan Journal of Mechanical and Industrial Engineering. All rights reserved

Keywords: FDM process, SCFR-PLA, mechanical properties, thermal investigation, SEM analysis.

1. Introduction

In current years, significant advancements in engineering methods have addressed the enhancement of material properties with optimizing manufacture costs. This equilibrium is essential for growing the usefulness of diverse materials in various engineering fields, achieving both performance and optimized cost are required. For that, important progressions in engineering study has been addressed to evolving the mechanical characterization of studied materials and improving their properties through both experimental and numerical methods [1–3]. This consist of optimizing and understanding the effect of manufacturing parameters on material properties. The main goal is to ameliorate the strength and the efficiency of materials [4–6].

Among recent developments, 3D printing technologies of thermoplastics has been widely used for prototyping due to its flexibility and efficiency. Particularly, Fused Deposition Modeling (FDM) is the most usually used as 3D printing technique, distinguished by its high reliability, a wide variety of low-cost filament material availability, and speedy prototyping abilities [7,8]. In this context, Patpatiya et al. [9] elaborated a comparative study of different 3D printing technologies, highlighting FDM's cost advantages over other more costly processes. These advantages make FDM a favored choice over other 3D printing processes of materials based on polymers, mainly for prototyping and small-scale fabrication.

Varied studies have been conducted on using the FDM technique for printing polymer-based structures [10–12]. These studies focused on forecasting the mechanical properties of printed polymer parts under diverse printing

* Corresponding author e-mail: hamdi.hentati@yahoo.fr.

conditions. The influence of printing parameters on mechanical strength was explored in order to optimize the FDM method and increase material properties. Indeed, Hsueh et al. [13] examined the influence of printing parameters on PLA and PETG materials under different loading conditions. They showed that the higher printing temperatures enhanced the mechanical properties of both thermoplastics, with PLA revealing higher strength while PETG showed lower thermal deformation. In the same framework, Hsueh et al. [14] proposed a computational model to predict the mechanical characteristics and mesostructure of ABS polymers, which printed via FDM method. A parametric analysis determines the effect of 3D printing parameters on thermoplastic properties, allowing the design of optimized printed components. In addition, Alzyod and Ficzer [15] studied the impact of diverse printing methods on the ultimate tensile strength (UTS) of printed PLA specimens through experimental and statistical analyses.

Recently, diverse studies have been conducted to explore the reinforcement of thermoplastic matrices with fillers such as short/continuous fibers and nanoparticles. In fact, pure polymers, which are printed by using FDM method, suffers from limited mechanical characteristics, which significantly constrains their usefulness in diverse engineering applications. To overcome these restrictions, researchers have explored the reinforcement of thermoplastic matrices. Thermal and mechanical behavior of printed thermoplastic composites using FDM technique were investigated in several studies. However, this technique still requires further improvements to refine its parameters and enhance the dimensional and surface quality of printed parts.

Ferreira et al. [16] examined the thermal stability, the mechanical characteristics, and the microstructural properties of printed PETG polymers and the short fiber reinforcement PETG composites. They demonstrated that the FDM parameters and fiber content influence considerably the thermal, mechanical, and microstructural properties of these printed parts. Similarly, Ammar et al. [17] analyzed the effects of 3D printing parameters, which are raster angle, printing speed, and extrusion temperature on the mechanical properties of FDM-printed thermoplastics reinforced with carbon fiber. Findings show that the higher printing speed increases porosity, decreasing then the stiffness of printed composites. Higher extrusion temperature increases their strength and their ductility by improving layer adhesion and minimizing porosity, as proved by SEM analysis. Within this context, Juan et al. [18] explored continuous carbon fiber-reinforced PLA (CCFR-PLA) for hip prosthetic implants. Thermal and structural characterizations of printed parts revealed chemical interactions between polymer and continuous fibers that affected the composite's thermal response.

Furthermore, other studies have elaborated the use of Kevlar, carbon, and glass fibers to increase the mechanical properties of FDM-printed thermoplastics. Among these reinforced fibers, the carbon has the high-performance due to its excellent mechanical strength and low density. It is characterized also by its resistance to corrosion and wear, its high thermal and electrical conductivity, its low thermal expansion, and its distinctive piezoresistive behavior as showed in the following works [19-21]. Then, carbon fiber reinforced thermoplastic composites are widely used in the aerospace and automotive industries due to these superior performance and lightweight characteristics [22].

Consequently, short carbon fiber-reinforced PLA (SCFR-PLA) composites have appeared as a promising solution, offering a balance between strength, stiffness, and 3D printing process ability. The addition of short carbon fibers improves the mechanical properties of PLA, making it more suitable for diverse engineering applications [23,24]. However, achieving best mechanical and microstructural properties requires a thorough understanding of the influence of 3D printing process parameters, including carbon fiber content, raster angle, printing speed, and layer thickness.

Our study explores the influence of these key parameters on the mechanical, thermal, and microstructural properties of SCFR-PLA composites printed via FDM. Findings show that low raster angles and layer thicknesses enhance stiffness and strength, while higher printing speeds increase strength but reduce stiffness. The addition of short carbon fibers further improves mechanical performance, though with reduced ductility. TGA and SEM analyses support these results by revealing improved thermal stability and a clear relationship between porosity and mechanical behavior. Compared to the recent studies in the literature, our findings confirm the effect of FDM parameters on mechanical performance. However, some limitations remain, including the lack of fatigue and impact testing to assess long-term performance.

2. Experimental Setup

2.1. Matrix material

Polymers and composites may be printed by using the FDM technology. In this context, the most widely utilized polymers as matrix for printed composites are acrylonitrile butadiene styrene (ABS), polylactic acid (PLA), and polyamide (PA) [25]. We elaborate a comparative study of the mechanical properties, in terms of the ultimate tensile strength (UTS) and the tensile modulus (E) of these polymers based on the main results elaborated by the following works [12,25-30]. Figure 1 illustrated the main results of the 3D-printed polymer materials: ABS, PLA, and PA with different FDM parameters.

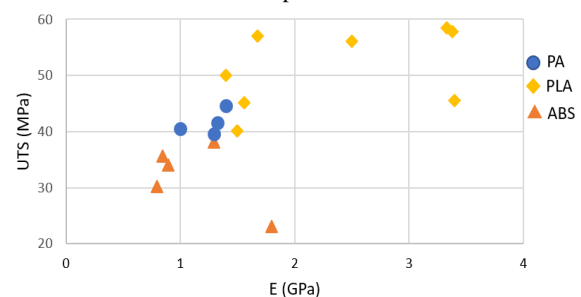


Figure 1. UTS and E variation of FDM-Printed Polymer Specimens [12,25-30]

PLA has the highest tensile modulus and a relatively high ultimate tensile strength. This indicates that PLA has a higher rigidity and strength compared to ABS and PA. For that, PLA is considered as the best choice, among the three polymers, as matrix materials in printed composites for applications needing high mechanical properties.

2.2. FDM parameters

In this study, we use the PLA and short carbon fiber-reinforced PLA (SCFR-PLA) composites to print tensile

specimens. The geometry of these specimens are in accordance with the ASTM D638 standard. FDM process begins with the continuous feeding of filament from the spool of PLA or SCFR-PLA into the extruder system. Within this system, the filament is heated to a semi-molten state before being extruded through a high-temperature nozzle. This molten material is then accurately put on the print bed,

forming the first layer of the specimen. The print bed and extruder system allow the deposition layer by layer until the complete 3D specimen is printed. Table 1 presents the properties of the printed polymer and composites parts as indicated in their technical data sheets.

Table 1. Properties of printed filaments

	PLA	SCFR-PLA	
Short carbonfiber content (%)	0	15	30
Density (g/cm ³)	1.24	1.3	1.32

The 3D printing settings through the printing process are as follows: the nozzle diameter is 0.4mm, the filament diameter is 1.75 ± 0.05 mm, the infill percentage is 100%, the extrusion width is 1.28mm, and the extrusion and the bed temperatures are 210°C and 60°C respectively. The diameter of the carbon fibers is around 7-9 μ m and the length is 100 μ m.

However, we vary the main parameters, which affect the mechanical properties of printed parts. Indeed, three raster angles (θ) were chosen for the printing orientation. Each raster angle was applied at two levels for each printing speeds (V) and layer thicknesses (Th). Three levels of short carbon fiber reinforcement (%C). The different levels of these factors are given in Table 2.

Table 2. FDM printing settings

3D printing settings			Carbonfiber content %C (%)
θ (°)	V (mm/s)	Th (mm)	
0 – 45 – 90	25 – 50	0.3 – 0.4	0 – 15 – 30

2.3. Mechanical tests

To analyze the influence of carbon fiber content (%C) and the FDM parameters on the mechanical properties of the printed parts, pure PLA and SCFR-PLA samples were submitted to tensile test until failure at room temperature (Figure 2). Tensile tests were performed using a universal testing machine at a constant strain rate of 2 mm/min. An extensometer was used in each tensile test to accurately measure the elongation of the examined parts. Three measurements were performed on each tensile test and the average values was used to construct the stress-strain curves.

Mechanical properties were deduced from the experimental stress-strain curves for each set of the selected FDM parameters.

In addition, micro-hardness tests are elaborated. Micro-hardness tests are conducted using the Vickers micro-hardness (Figure 3) with a load of 0.5 kg (HV0.5) with a dwell time of 20 seconds.



Figure 2. Experimental set-up of tensile test

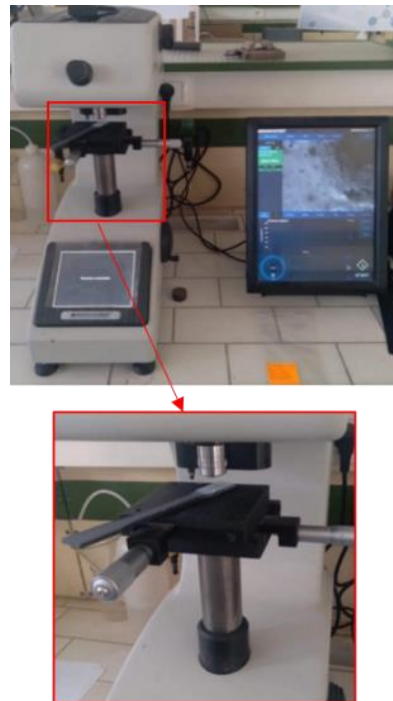


Figure 3. Experimental set-up of micro-hardness test

Three values of micro-hardness were measured and the average value was taken.

2.4. Thermal and microstructural analysis

The thermal stability of the printed composites as function of printing speed was investigated by thermogravimetric analysis (TGA). These measures were realized using a Mettler Toledo thermogravimetric analyzer (figure 4). A heating scan from 0°C to 800 °C was performed under nitrogen atmosphere at a rate of 10 °C/min.



Figure 4. Thermogravimetric analyzer (TGA)

Scanning electron microscopy (SEM-QUANTA FEG-250) was also used in order to examine the microstructural behavior of the fractured surfaces of printed parts (figure 5).

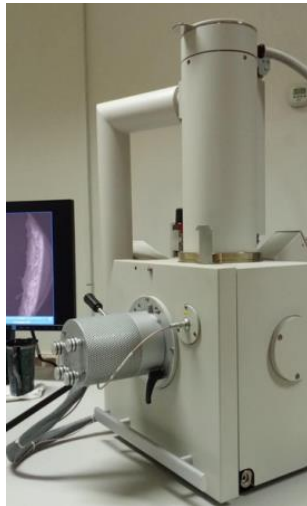


Figure 5. Scanning Electron Microscope (SEM)

The SEM is an advanced imaging tool equipped with an electron beam that scans the surface of a specimen to generate high-resolution images. It offers detailed topographical and morphological analysis by detecting secondary or backscattered electrons.

3. Results and Discussions – Mechanical tests

We represent in Figure 6 different tensile stress-strain curves of printed composites at various carbon fiber contents (%C), raster angles (θ), layer thickness (Th), and printing speeds (V). We show that the variation of these FDM parameters significantly affect the mechanical properties of printed parts. Therefore, it is interesting to understand their influence principally on Young modulus (E), ultimate tensile strength (UTS), and yield strength (YS).

3.1. Evolution of Young's modulus (E)

As illustrated in Figure 7, the Young's modulus (E) varies with the FDM parameters, which are θ , V, Th, and %C.

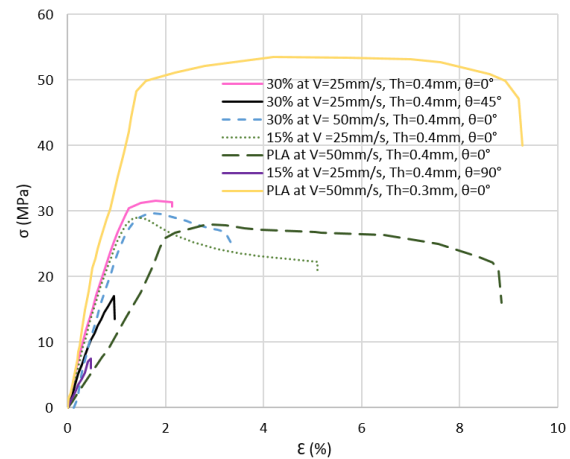


Figure 6. Tensile stress-strain curves of SCFR-PLA at different FDM parameters

We show that the rigidity decreases with growing θ and V. Best stiffness is achieved at $\theta=0^\circ$. This result is in agreement with findings by Ammar et al. [17] on carbon fiber reinforced PETG. Particularly, for %C=30%, the printed SCFR-PLA at low speed shows the highest Young's modulus (E) at $\theta=0^\circ$, indicating superior rigidity. However, for %C=30%, the printed SCFR-PLA exhibits brittle behavior, which is a significant drawback. Despite its enhanced rigidity, this brittleness can limit its usefulness if toughness and durability properties are required. Moreover, increasing Th consistently decreases stiffness in printed parts. The effect of short carbon fiber reinforcement on the rigidity is important; comparing pure PLA (%C=0%) to composite with %C=15%, the adding of short carbon fibers augments rigidity independent of V. Based on these findings, we show that the material rigidity is inversely proportional to θ , V and Th, while it varies directly with %C.

3.2. Evolution of ultimate tensile strength (UTS)

Figure 8 illustrates the variation of ultimate tensile strength (UTS) as a function of θ , V, Th, and %C.

A significant decrease of 65% in UTS is measured when θ rises from $\theta=0^\circ$ to $\theta=90^\circ$ for %C=15% parts printed at V=50mm/s. In fact, for Th=0.3 mm, V=50 mm/s, and %C=15%, the UTS decreases from 61MPa at 0° to 20MPa at 90° , which is a 67.2% decrease.

For Th = 0.4 mm, V=50 mm/s, and %C=15%: UTS drops from 30.13MPa at 0° to 10.44MPa at 90° , a 65.3% decrease. The influence of V is negligible for samples printed at 0° , whereas for $\theta=45^\circ$ and $\theta=90^\circ$, increasing V enhances UTS, mainly for Th=0.3mm. This improvement is attributed to stronger interlayer bonding at higher print speeds, as successive layers are deposited with a shorter interval, reducing cooling time and improving adhesion between layers [31]. Furthermore, for $\theta=45^\circ$ and $\theta=90^\circ$, increasing %C from %C=15% to %C=30% leads to improved tensile strength, highlighting the reinforcing effect of short carbon fibers. About the influence of Th, it is clear that increasing Th from Th=0.3mm to Th=0.4mm significantly reduces UTS, particularly at $\theta=0^\circ$. This outcome is consistent with previous studies by Nomani et al. [32] for printed ABS and Ajay et al. [33] for carbon fiber-reinforced PETG. The role of %C is further

emphasized, as the integration of carbon fibers into the thermoplastic matrix outcomes in a considerable increase in UTS, enhancing both the durability and mechanical performance of the printed composites under tensile loading. Additionally, Adil and Lazoglu [34] validated that UTS and the compressive strength could be further improved by utilizing carbon fiber-reinforced polymers, which offers higher structural performance. The findings in this subsection make known that UTS decreases with growing θ and Th , while it increases with V and $\%C$.

In addition, the maximum UTS of 78MPa is measured at optimal conditions: $\theta = 0^\circ$, $Th=0.3\text{mm}$, $V=30\text{mm/s}$, and $\%C=15\%$, highlighting the strong influence of fiber alignment and reinforcement. In contrast, the minimum UTS of 4.9MPa occurs under the least favorable conditions, which are $\theta=90^\circ$, $Th=0.4\text{mm}$, $V=70\text{mm/s}$, and $\%C=0\%$ highlighting the negative effects of poor fiber orientation, higher layer thickness, faster speed, and absence of carbon reinforcement.

3.3. Evolution of Yield strength (YS)

Figure 9 illustrates the variation of yield strength (YS) as a function of FDM parameters.

A significant decrease of approximately 65% in YS is observed as θ increases from $\theta=0^\circ$ to $\theta=90^\circ$ for 15% SCFR-PLA printed at $V=50\text{ mm/s}$. Additionally, increasing $\%C$ from 15% to 30% in composite structures leads to a notable enhancement in YS, particularly at $\theta=45^\circ$ and $\theta=90^\circ$, highlighting the reinforcing effect of short carbon fibers. It is important to note that V has a negligible impact on YS in this case. However, a consistent decline in YS is observed with an increase in Th from $Th=0.3\text{mm}$ to $Th=0.4\text{mm}$, as well as when $\%C$ increases from $\%C=0\%$ to $\%C=15\%$. This degradation in mechanical properties is mainly related to the stiffening effect of carbon fiber reinforcement, which limits the elasticity of the pure polymer matrix, thereby reducing its ability to deform plastically before yielding. In this context, Ning et al. [35] showed that increasing carbon fiber content generally decreases the yield strength of the composite compared to ABS polymer printed via FDM. While a slight increase occurs at $\%C=5\%$, the experimental result indicates reduced yield strength as fiber content rises, particularly beyond $\%C=10\%$. The maximum yield strength is observed in the ABS polymer part.

The obtained results clearly show an inverse proportional relationship between YS and θ , Th and $\%C$, with no notable influence of V .

3.4. Evolution of micro-hardness (HV0.5)

The micro-hardness (HV0.5/20s) is measured at 0.5 kgf with a dwell time of 20 seconds. The Vickers micro-hardness (HV) of 3D-printed SCFR-PLA composites is influenced by FDM process parameters (Figure 10), with carbon fibre content, printing speed, raster angle, and layer thickness being particularly significant.

The micro-hardness of PLA composites increases when adding carbon fiber content ($\%C=15\%$) as the reinforcement in the PLA matrix. However, an increase of $\%C$, specifically at $\%C=30\%$, a decrease in hardness is

observed. This reduction is attributed to the formation of microscopic voids, which slightly decrease the composite's density and limit further hardness improvements. This trend is consistent with the findings of Wang et al. [36], who reported a similar relationship between excessive fiber content and the presence of structural defects affecting hardness performance of printed composite.

A layer thickness of $Th=0.3\text{mm}$ enhances interlayer adhesion by promoting better bonding between successive layers, thereby reducing defects and improving the overall hardness of the printed composite. However, using thicker layers can lead to increased porosity within the structure, which weakens the material by reducing density and compromising hardness but increases print time. Vorkapić et al. [37] investigated the effect of different printing parameters and heat treatments on PLA specimens. They found that thicker layers ($Th=0.2\text{mm}$) generally resulted in higher microhardness values compared to thinner layers ($Th=0.1\text{mm}$) after heat treatment, indicating a relationship between layer thickness and hardness. In order to validate our findings, we show the main results developed by Muhamedagić et al. [38]. In fact, they used carbon fiber-reinforced PLA composites with $Th=0.1\text{mm}$ and $\%C=5\%$ and $\%C=10\%$. They found that $V=40\text{mm/s}$ gives the accurate interlayer adhesion, then the best balance between efficiency and quality was showed. However, for $V=60\text{mm/s}$, the porosity is increased, while for $V=20\text{ mm/s}$, moderately decrease was illustrated for the composite's hardness. For our composites, we conducted micro-hardness tests with speeds neighboring to this optimal value. Indeed, we use two printing speeds: one higher than $V=20\text{mm/s}$ and one lower than $V=60\text{mm/s}$. We observed that for $V=25\text{mm/s}$, the best Vickers micro-hardness is measured compared to $V=50\text{mm/s}$. This speed ensures optimal interlayer bonding, enhancing micro-hardness of SCFR-PLA.

However, at $V=50\text{mm/s}$, this speed weakens layer adhesion, leading to increased porosity and decreased micro-hardness.

Varying the raster angle slightly influenced the hardness of the PLA material. The average hardness of SCFR-PLA printed by FDM essentially follows a linear relationship, increasing slightly as the raster angle increases. Micro-hardness measurements, taken from the perimeter layer of the specimens, show a rise in values with the increase in the raster angle. This is because, as the printing angle grows, the layers become more parallel to the loading direction, affecting the micro-hardness measurements. This increasing linear relationship between raster angle and hardness response was proved by Zeng et al. [39] for thermoplastic parts printed via FDM. In addition, when the layer thickness is 0.3mm, the variation in raster angle affects the hardness more significantly and visibly. This is for the reason that there are more interfaces between layers, making the hardness more sensitive to the raster angle.

3.5. Statistical analysis of measured properties

We conducted three measurements per test condition. We calculate in this section the standard deviation (SD) to statistically validate the influence of your FDM parameters

(θ , %C, Th, V) on the mechanical properties (E, UTS, YS, HV). In fact, SD is calculated using equation 1.

$$SD = \sqrt{\frac{1}{2} \sum_{i=1}^3 (X_i - \hat{X})^2} \quad (1)$$

Where \hat{X} is the average value of each measured property X_i .

SD values remain relatively low, showing good repeatability of the measurements. Precisely, SD(E) ranges between 20 and 150 MPa, SD(UTS) between 2 and 14 MPa, SD(YS) between 2 and 10 MPa, and SD(HV) between 1 and 5 HV.

However, higher SD values are mainly obtained for raster angles $\theta=45^\circ$ and 90° . In fact, at $\theta=45^\circ$, the oblique fiber orientation induces combined shear and tensile stresses, which are sensitive to slight variations during printing. At $\theta=90^\circ$, the loading direction is perpendicular to the printed layers, making the mechanical response highly dependent on interlayer adhesion. Increased

variability of SD is also observed at a higher printing speed ($V=50\text{mm/s}$), where limited fusion time between layers reduce mechanical rigidity and strength, and at a larger layer thickness ($\text{Th}=0.4\text{mm}$), which reduces the number of fusion interfaces and may result in lower cohesion. In contrast, finer layers ($\text{Th}=0.3\text{mm}$) offer better fusion, leading to lower SD values. In addition, at 0% carbon fiber content, the printed PLA behaves more homogeneously, showing minimal variability. In conclusion, maximum SD values are observed in the following cases:

- SD(UTS) up to 14MPa at $\theta=90^\circ$, %C = 15%, $V=50\text{ mm/s}$, $\text{Th}=0.4\text{ mm}$.
- SD(E) up to 150MPa at $\theta=45^\circ$ and 90° .
- SD(YS) up to 10MPa at $V=50\text{ mm/s}$, $\text{Th}=0.4\text{mm}$, and $\theta=45^\circ$ and 90° .
- SD(HV) up to 5 HV at %C = 30% and $\text{Th}=0.4\text{mm}$.

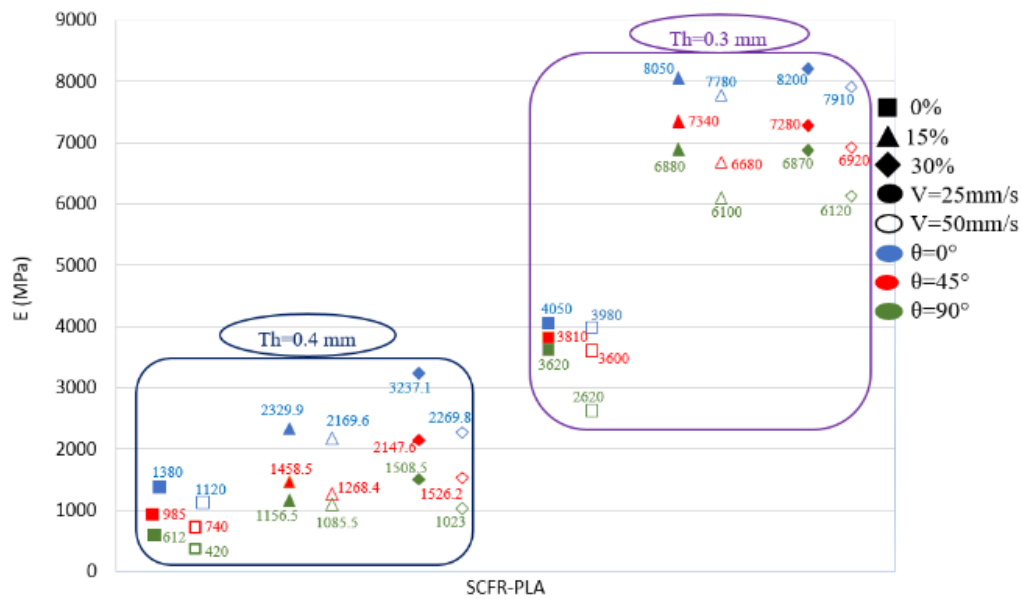


Figure 7. Relationship between E and FDM parameters

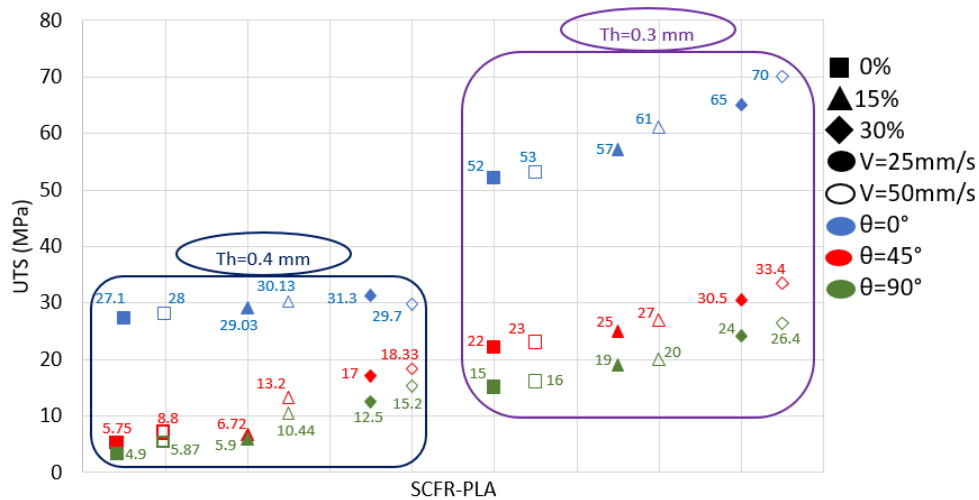


Figure 8. Relationship between UTS and FDM parameters

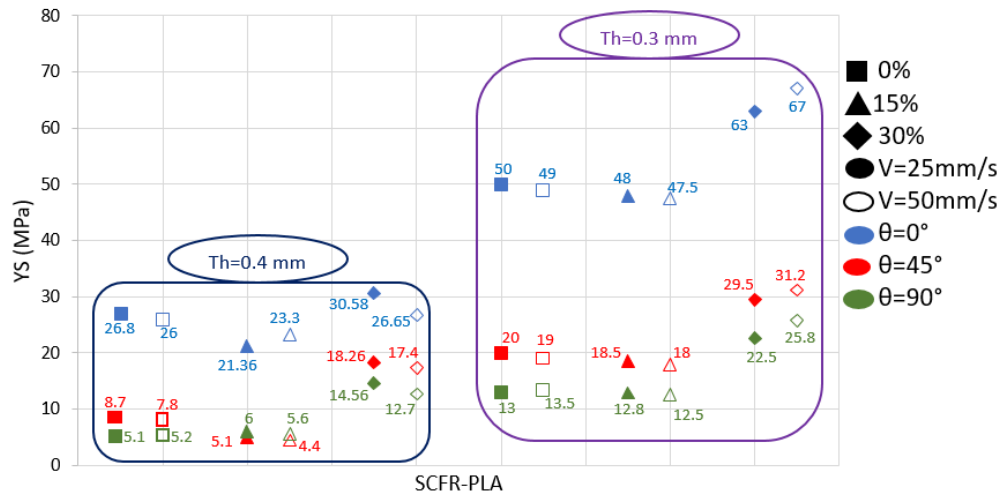


Figure 9. Relationship between YS and FDM parameters

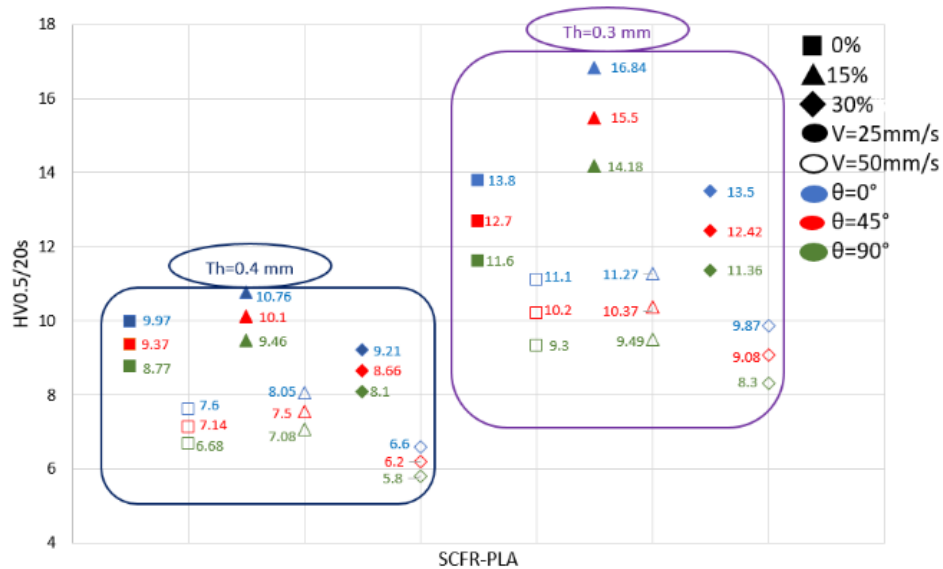


Figure 10. Dependence of Vickers micro-hardness on FDM parameters

4. Results and Discussions – Thermal and microstructural analyses

To investigate the influence of temperature on the weight change of printed composites, we illustrate in Figure 11 the obtained thermogravimetric curves and we show that %C=30% for SCFR-PLA composite parts had a thermal degradation in a single step.

In fact, we conducted the TGA under controlled atmospheric conditions. TGA is a widely used technique for assessing the thermal behavior of materials, providing insights into properties such as thermal stability, decomposition temperature, and the degree of weight loss during thermal decomposition. Moreover, TGA allows for the identification of the exact temperature at which material degradation begins and enables the quantification of degradation at various temperatures. In this section, TGA was performed to evaluate the impact of V on the thermal stability of %C=30% of SCFR-PLA composite. Studying the influence of this parameter on thermal behavior is critical, especially when the composite is

subsequently employed in high-temperature applications. These findings agree with the degradation of the PLA matrix [40].

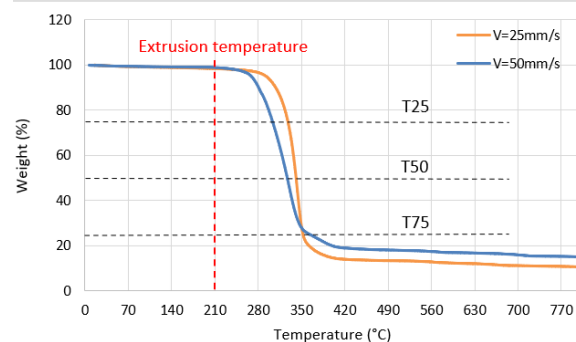


Figure 11. TGA thermograms of 30%SCFR-PLA at various V

For V=25mm/s, the thermal degradation starts at 320°C and a residue of 10.47%wt was still present at the end of the experiment. For a higher printing speed of V=50mm/s, the initial temperature of thermal degradation decreased to 287°C with a residue of 14.85%. This result suggests that faster printing speed may accelerate the thermal

degradation of the printed parts in terms of mass loss. In contrast, regarding the final degradation temperature, it was greater at $V=50\text{mm/s}$. Table 3 presents the temperatures at which the samples experience weight losses of 25%, 50%, and 75% relatively to their initial weights (T25, T50, and T75, respectively).

Table 3. TGA results of 30%SCFR-PLA at various printing speeds (V)

	V=25mm/s	V=50mm/s
Transition temperature (start) (°C)	320	287
Transition temperature (finish) (°C)	353	348
T25 (°C)	327.54	303.38
T50 (°C)	340.78	325.10
T75 (°C)	352.03	357.12
Residual mass (%)	10.47	14.85

The early thermal degradation is exhibited particularly at T25 and T50. The 3D printing process uses a fixed extrusion temperature (210°C). Under the printing conditions, high printing speeds may induce significant thermal degradation of the material structure during printing composite part. Such thermal stress can undesirably affect component integrity and mechanical properties, resulting decrease print quality and enhanced failure, which decreases the durability of printed part.

These findings highlight the necessity of optimizing printing speed for SCFR-PLA to achieve an optimal equilibrium between 3D printing cost and mechanical performance. This research is particularly relevant for applications involving high-temperature environments, where material stability and thermal resistance are essential for ensuring durability of printed components.

To well understand these results, the fracture surfaces, after tensile tests, of the 30%SCFR-PLA, printed at various V, $\theta=0^\circ$ and $Th=0.4\text{mm}$, were examined using SEM analysis. The SEM images are presented in Figure 12.

The increase of the printing speed promotes the presence of wide air pores within the printed composite. The increased print speed limits proper melting and layer consolidation, subsequently degrading mechanical properties. This effect is showed by the reduction in the rigidity of composite, as observed during mechanical testing. This finding highlights the importance of optimizing the balance between printing speed, then the production cost, and print quality to achieve strong layer adhesion.

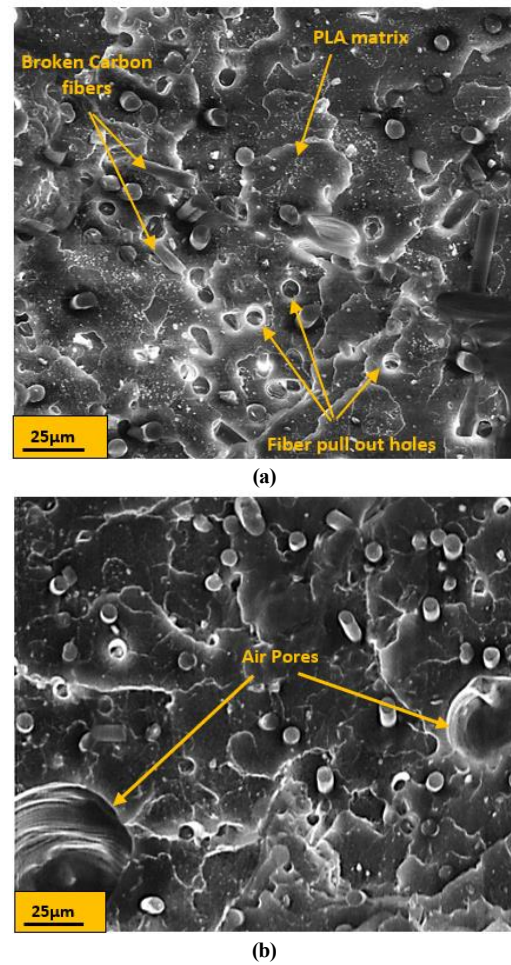


Figure 12. SEM images of damaged surfaces in 30%SCFR-PLA parts, $\theta=0^\circ$ and $Th=0.4\text{mm}$, (a) $V=25\text{mm/s}$. (b) $V=50\text{mm/s}$.

5. Conclusion

In this study, SCFR-PLA parts were printed using the FDM technique under varying printing speeds (V), raster angles (θ), and layer thicknesses (Th). The carbon fiber content (%C) ranged from 0% (pure PLA) to 30%. Through tensile testing, key mechanical properties, including Young's modulus (E), ultimate tensile strength (UTS), and yield strength (YS), were evaluated.

The obtained results were supported by thermal and microstructural characterizations using TGA and SEM observations, respectively. The main conclusions of this study are as follows:

- Material stiffness, identified by E, is inversely proportional to θ , V and Th, but increases directly with %C.
- UTS decreases with increasing θ and Th, while it increases proportionally with both V and %C.
- YS shows an inverse relationship with θ , Th and %C, with V having no significant impact.
- The micro-hardness results highlight an inverse proportional relationship between HV and Th, and V. As these parameters increase, the hardness decreases, likely due to reduced bonding strength between layers and increased porosity in the printed structure.
- The micro-hardness (HV) values obtained indicate a linear relationship with the raster angle (θ). When the

layers are more parallel, the force is absorbed more efficiently within each layer, leading to higher hardness. For this reason, the highest values are observed at $\theta = 90^\circ$. In contrast, $\theta = 0^\circ$ shows lower hardness values.

- Regarding the influence of %C, the reinforcement significantly enhances the micro-hardness of the SCFR-PLA composites, particularly at %C = 15%, where the added fibers contribute to improved structural integrity and load-bearing capacity. However, at %C = 30%, a decrease in hardness is observed. The excessive fiber content increases voids.
- The effect of V on print quality is closely associated with porosity within the printed structures.

The lack of fatigue and impact testing to assess long-term performance remains a main limitation of this work. Future work should address these aspects and explore hybrid reinforcements to further enhance the mechanical performance and reliability of printed composites.

Author contribution

All authors contributed to the research, writing, and reviewing of the paper.

Declarations

Funding: The authors received no financial support for the research, authorship, and/or publication of this article.

Ethics approval: Not applicable. Consent to participate: Not applicable.

Consent for publication: The authors give all the rights to publish the material presented in this work.

Competing interests: The authors declare no competing interests.

References

- [1] S. G. Ghalme, G. Sachin, "Improving Mechanical Properties of Rice Husk and Straw Fiber Reinforced Polymer Composite through Reinforcement Optimization". Jordan Journal of Mechanical and Industrial Engineering, Vol. 15, No. 5, 2021, pp.411 - 417.
- [2] C. Hammami, N. Kammoun, H. Hentati, et al., "Parametric analysis of the damage characterization tests of aluminum bulk material". Journal of Mechanical Science and Technology, Vol. 36, 2022, pp.5019-5025. DOI:10.1007/s12206-022-0914-z.
- [3] S. Moakhar, H. Hentati, M. Barkallah et al., "Modeling of the ductile damage—application for bar shearing". MaterialwissWerkstofftech, Vol. 50, 2019, pp.1353-1363. <https://doi.org/10.1002/mawe.201800128>.
- [4] M. Soori, M. Asmael, "A review of the recent development in machining parameter optimization". Jordan Journal of Mechanical and Industrial Engineering, Vol. 16, No. 2, 2022, pp.205-223.
- [5] B. Ben Fraj, T. Kamoun, H. Hentati et al., "Optimization of forming force and Erichsen index using Taguchi design of experiments: Mathematical models and experimental validation", Proc. Inst. Mech. Eng. Part B. Vol. 238, No. 9, 2024, pp.1316-1326. DOI:10.1177/09544054231194107.
- [6] R. Venkatesh, "Machining parameter optimization and study the turning operation behaviour of hybrid Al/Mg composites". Jordan Journal of Mechanical and Industrial Engineering, Vol. 18, No. 4, 2024, pp.711-719. <https://doi.org/10.59038/jjmie/180407>.
- [7] D. G. Zisopol, M. Tănase, A. I. Portoacă, "Innovative Strategies for Technical-Economical Optimization of FDM Production", Polymers. Vol. 15, 2023, pp.3787. <https://doi.org/10.3390/polym15183787>.
- [8] I. Portoacă, M. Tănase, "Exploring Shore D Hardness Variations Under Different Printing Conditions and Post-processing Treatments", Jordan Journal of Mechanical and Industrial Engineering, Vol. 18, No. 2, 2024, pp.421-429. <https://doi.org/10.59038/jjmie/180214>.
- [9] P. Patpatiya, K. Chaudhary, A. Shastri et al., "A review on polyjet 3D printing of polymers and multi-material structures". Proc. Inst. Mech. Eng. Part C, Vol. 236, No. 14, 2022, pp.7899-7926. DOI:10.1177/09544062221079506.
- [10] T. Yao, Z. Deng, K. Zhang, et al., "A method to predict the ultimate tensile strength of 3D printing polylactic acid (PLA) materials with different printing orientations", Composites Part B: Engineering, 163, 2019, pp.393–402.
- [11] O. Luzanin, D. Movrin, V. Stathopoulos, et al., "Impact of processing parameters on tensile strength, in-process crystallinity and mesostructure in FDM-fabricated PLA specimens", Rapid Prototyping Journal, Vol. 20, 25, 2019, pp.1398–1410.
- [12] M. A. Seidl, J. L. Safka, J. L. Bobek, et al., "Mechanical properties of products made of ABS with respect to individuality of FDM production processes", Modern Machinery Sciences Journal, Vol. 2, 2017, pp.1748–1751.
- [13] MH. Hsueh, CJ. Lai, SH. Wang, et al. "Effect of Printing Parameters on the Thermal and Mechanical Properties of 3D-Printed PLA and PETG, Using Fused Deposition Modeling". Polymers, Vol. 13, No. 11, 2021, pp.1758. DOI:10.3390/polym13111758.
- [14] S. Garzon-Hernandez, D. Garcia-Gonzalez, A. Jérusalem, et al., "Design of FDM 3D printed polymers: An experimental-modelling methodology for the prediction of mechanical properties", Materials & Design, Vol. 188, 2020, pp.108414.
- [15] H. Alzyod, P. Ficzer, "The Influence of the Layer Orientation on Ultimate Tensile Strength of 3D Printed Polylactic Acid", Jordan Journal of Mechanical and Industrial Engineering, Vol. 16, No.3, 2022.
- [16] Ferreira, D. Vale, M. Machado, et al., "Additive manufacturing of polyethylene terephthalate glycol /carbon fiber composites: An experimental study from filament to printed parts". Proc. Inst. Mech. Eng. Part L, Vol. 233, No. 9, 2019, pp.1866-1878. DOI:10.1177/1464420718795197
- [17] S. Ammar, B. Ben Fraj, H. Hentati et al., "Mechanical performances of printed carbon fiber-reinforced PLA and PETG composites". Proc. Inst. Mech. Eng. Part L J. Mater. Des. Appl. Vol. 238, 2024, pp.1488–1499.
- [18] P. G. Juan, V. S. Carlos, J. V. G. Luis, et al., "Structural composite based on 3D printing polylactic acid/carbon fiber laminates (PLA/CFRC) as an alternative material for femoral stem prosthesis", Journal of the Mechanical Behavior of Biomedical Materials, Vol. 138, 2023, pp.105632. DOI: 10.1016/j.jmbbm.2022.105632.
- [19] S. S. Yao, F. L. Jin, K. Y. Rhee, et al., "Recent advances in carbon-fiber-reinforced thermoplastic composites: A review", Composites Part B: Engineering, Vol. 142, 2018, pp.241–250.
- [20] R. Omer, H. S. Mali, S. K. Singh, "Tensile performance of additively manufactured short carbon fibre-PLA composites: Neural networking and GA for prediction and optimization", Plastics, Rubber and Composites: Macromolecular Engineering. Vol. 49, No. 6, 2020, pp.1–10.
- [21] SH. Saneii, A. Arndt, R. Doles, "Open hole tensile testing of 3D printed continuous carbon fiber reinforced composites". Journal of Composite Materials, Vol. 54, No 20, 2020, pp.2687-2695.

- [22] N. Van de Werken, H. Tekinalp, P. Khanbolouki, et al., "Additively Manufactured Carbon Fiber-Reinforced Composites: State of the Art and Perspective". *Additive Manufacturing*, Vol. 31, 2019, pp.100962.
- [23] Sunil, A. Roberto, J. G. Douglas, "Enhancing the interlayer tensile strength of 3D printed short carbon fiber reinforced PETG and PLA composites via annealing". *Additive Manufacturing*, Vol. 30, 2019, pp.00922. DOI:10.1016/j.addma.2019.100922
- [24] M. Saleh, S. Anwar, A. M. Al-Ahmari, et al., "Prediction of Mechanical Properties for Carbon fiber/PLA Composite Lattice Structures Using Mathematical and ANFIS Models", *Polymers* Vol.15, 2023, pp.1720. <https://doi.org/10.3390/polym15071720>.
- [25] S. Wickramasinghe, T. Do, P. Tran, "FDM-Based 3D Printing of Polymer and Associated Composite: A Review on Mechanical Properties, Defects and Treatments". *Polymers*, Vol. 12, No 7, 2020, pp.1529. doi:10.3390/polym12071529.
- [26] M. S. Priya, K. Nareesh, R. Jayaganthan, et al., "A comparative study between in-house 3D printed and injection molded ABS and PLA polymers for low-frequency applications", *Materials Research Express*, Vol. 6, 2019, pp.085345.
- [27] M. Samykano, S. K. Selvamani, K. Kadirgama, et al., "Mechanical property of FDM printed ABS: Influence of printing parameters". *International Journal of Advanced Manufacturing Technology*, 12, 2019, 2779–2796.
- [28] M. Vinyas, S. J. Athul, D. Harursampath, et al., "Mechanical characterization of the Poly lactic acid (PLA) composites prepared through the Fused Deposition Modelling process". *Materials Research Express*, Vol. 6, 2019, pp.105359.
- [29] M. Lay, N. L. N. Thajudin, Z. A. A. Hamid, et al., "Comparison of physical and mechanical properties of PLA, ABS and nylon 6 fabricated using fused deposition modeling and injection molding". *Composites Part B: Engineering*, Vol. 176, 2019, pp.107341.
- [30] Rodríguez-Panes, J. Claver, A. M. Camacho, et al., "The influence of manufacturing parameters on the mechanical behaviour of PLA and ABS pieces manufactured by FDM: A comparative analysis". *Materials*, Vol. 11, 2018, pp.1333.
- [31] A. Ansari, M. Kamil, "Effect of print speed and extrusion temperature on properties of 3D printed PLA using fused deposition modeling process". *Materials Today*, Vol. 45, No. 6, 2021, pp.5462-5468. DOI:10.1016/j.matpr.2021.02.137
- [32] J. Nomani, D. Wilson, M. Paulino, et al., "Effect of layer thickness and cross-section geometry on the tensile and compression properties of 3D printed ABS", *Materials Today Communications*, Vol. 22, 2019, pp.100626.
- [33] K. Ajay, M. S. Khan, S. B. Mishra, "Effect of machine parameters on strength and hardness of FDM printed carbon fiber reinforced PETG thermoplastics", *Materials Today*, Vol. 27, No. 2, 2020, pp.975-983. DOI:10.1016/j.matpr.2020.01.291
- [34] S. Adil, I. Lazoglu, I. "A review on additive manufacturing of carbon fiber-reinforced polymers: Current methods, materials, mechanical properties, applications and challenges", *Journal of Applied Polymer Science*, Vol. 140, No. 7, 2023, pp.e53476.
- [35] F. Ning, W. Cong, J. Qiu, et al., "Additive manufacturing of carbon fiber reinforced thermoplastic composites using fused deposition modeling". *Composites Part B: Engineering*, Vol. 80, 2015, pp.369–378.
- [36] Wang, X. Tang, Y. Zeng, et al., "Carbon Fiber-Reinforced PLA Composite for Fused Deposition Modeling 3D Printing", *Polymers*, Vol. 16, 2024, pp.2135.
- [37] M. Vorkapić, I. Mladenović, T. Ivanov, et al., "Enhancing mechanical properties of 3D printed thermoplastic polymers by annealing in moulds", *Advances in Mechanical Engineering*, Vol. 14, No. 8, 2022. doi:10.1177/16878132221120737
- [38] K. Muhamedagic, L. Berus, D. Potočnik, et al., "Effect of Process Parameters on Tensile Strength of FDM Printed Carbon Fiber Reinforced Polyamide Parts", *Applied Sciences*, Vol. 12, 2022, pp.6028. <https://doi.org/10.3390/app12126028>
- [39] Y. S. Zeng, M. H. Hsueh, C. J. Lai, et al., "An Investigation on the Hardness of Polylactic Acid Parts Fabricated via Fused Deposition Modeling", *Polymers*, Vol. 14, 2022, pp.2789. <https://doi.org/10.3390/polym14142789>
- [40] A. Pathek, J. R. F. Silva, D. D. Lima, et al., "Assessment of carbon fiber incorporation effects on overall characteristics and properties of 3D-printed PLA", *Journal of the Brazilian Society of Mechanical Sciences and Engineering*, Vol. 46, 2024, pp.640. DOI:10.1007/s40430-024-05233-x.